






## Article

# Fabrication and Characterization of $K_2CeCl_5/{}^6LiCl$ and $CeCl_3/SrCl_2/{}^6LiCl$ Eutectics for Thermal Neutron Detection

Ryuga Yajima <sup>1,2</sup> , Kei Kamada <sup>2,3,4,\*</sup>, Masao Yoshino <sup>3,4</sup>, Yui Takizawa <sup>1,2</sup>, Naoko Kutsuzawa <sup>4</sup>, Rei Sasaki <sup>1,2</sup> , Takahiko Horiai <sup>3,4</sup> , Rikito Murakami <sup>2,4</sup>, Kyoung Jin Kim <sup>2,4</sup> , Vladimir V. Kochurikhin <sup>4</sup>, Akihiro Yamaji <sup>3</sup>, Shunsuke Kurosawa <sup>2,3</sup>, Yuui Yokota <sup>2</sup> , Hiroki Sato <sup>3</sup>, Satoshi Toyoda <sup>3</sup>, Yuji Ohashi <sup>3</sup>, Takashi Hanada <sup>2</sup> and Akira Yoshikawa <sup>2,3,4</sup>

<sup>1</sup> Department of Materials Science, Graduate School of Engineering, Tohoku University, 6-6 Aramaki Aza Aoba, Aoba-ku, Sendai 980-8579, Miyagi, Japan

<sup>2</sup> Institute for Materials Research, Tohoku University, 2-1-1 Katahira, Aoba-ku, Sendai 980-8577, Miyagi, Japan

<sup>3</sup> New Industry Creation Hatchery Center, Tohoku University, 6-6-10 Aramaki Aoba, Aoba-ku, Sendai 980-8579, Miyagi, Japan

<sup>4</sup> C & A Corporation, 1-16-23, Itiban-tyo, Aoba-ku, Sendai 980-0811, Miyagi, Japan

\* Correspondence: kei.kamada.c6@tohoku.ac.jp; Tel.: +81-22-215-2214

**Abstract:** In recent years, thermal neutron detection using scintillators has been used in a wide range of fields. Thus, the development of scintillators with a higher light yield, faster decay, and higher sensitivity for thermal neutrons is required. In this study,  $K_2CeCl_5/{}^6LiCl$  and  $CeCl_3/SrCl_2/{}^6LiCl$  were developed as novel eutectic scintillators for thermal neutron detection.  $LiCl$  was selected as the neutron capture phase and  $K_2CeCl_5$  and  $CeCl_3$  were used as the scintillator phases. The eutectics of  $K_2CeCl_5/{}^6LiCl$  and  $CeCl_3/SrCl_2/{}^6LiCl$  were prepared using the Vertical Bridgman method and the phases were identified by scanning electron microscopy and powder X-ray diffraction measurements. The results of radioluminescence measurements under Ag source X-ray tube irradiation confirmed that the 5d-4f emission derived from  $Ce^{3+}$ . The cathodoluminescence spectra and thermal neutron responses of the prepared eutectics were measured to evaluate their optical properties.

**Keywords:** thermal neutron; scintillator; eutectic; crystal growth; vertical Bridgman (VB) method



**Citation:** Yajima, R.; Kamada, K.; Yoshino, M.; Takizawa, Y.; Kutsuzawa, N.; Sasaki, R.; Horiai, T.; Murakami, R.; Kim, K.J.; Kochurikhin, V.V.; et al. Fabrication and Characterization of  $K_2CeCl_5/{}^6LiCl$  and  $CeCl_3/SrCl_2/{}^6LiCl$  Eutectics for Thermal Neutron Detection. *Crystals* **2022**, *12*, 1795. <https://doi.org/10.3390/cryst12121795>

Academic Editors: Željka Antić and Aleksandar Ćirić

Received: 29 October 2022

Accepted: 8 December 2022

Published: 9 December 2022

**Publisher's Note:** MDPI stays neutral with regard to jurisdictional claims in published maps and institutional affiliations.



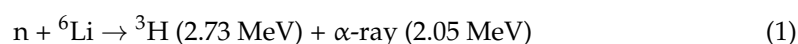
**Copyright:** © 2022 by the authors. Licensee MDPI, Basel, Switzerland. This article is an open access article distributed under the terms and conditions of the Creative Commons Attribution (CC BY) license (<https://creativecommons.org/licenses/by/4.0/>).

## 1. Introduction

Thermal neutrons have been increasingly used in fields such as medicine [1], homeland security [2], and crystallography [3]. For example, unlike X- and  $\gamma$ -rays, thermal neutrons have a higher penetrating power even through materials with high density and effective atomic number, in addition to their higher sensitivity to certain light elements (H, Li, etc.) [4,5]. Therefore, the use of neutron imaging of plastics and Li-ion batteries, which are difficult to image using X-rays, has attracted considerable attention in recent years [6].

To date,  ${}^3He$  gas counters have been the main method for thermal neutron detection [7].  ${}^3He$  has a high capture cross-section for thermal neutrons and its low effective atomic number and low sensitivity to  $\gamma$ -rays make it easy to distinguish thermal neutrons from  $\gamma$ -rays. However, because of the increasing demand for thermal neutron detection, the lack of  ${}^3He$  has become a concern, leading to the need for alternative methods.  $BF_3$  gas has been considered for thermal neutron detection, however its extreme toxicity has rendered  $BF_3$  as an unsuitable alternative [8].

Therefore, other detection methods using solid scintillators have been widely studied. Thermal neutrons can be detected via the nuclear transmutation reaction of  ${}^6Li$ -containing scintillators, which can be translated by Equation (1) [9].



An energy of 4.78 MeV, called the Q-value, is emitted by the triton and  $\alpha$ -ray. This high Q-value is expected to result in a high light yield from the scintillator. Several scintillators containing  $^6\text{Li}$  have been developed for thermal neutron detection. Among these, single-crystal scintillators such as  $\text{Eu, Ce:LiCaAlF}_6$  (LiCAF) [10,11], and  $\text{Ce:Cs}_2\text{LiYCl}_6$  (CLYC) [12] have been reported. However, it is difficult to improve the sensitivity of these single-crystal scintillators, which is important for neutron detection, because the  $^6\text{Li}$  concentration is restricted by their chemical formulas.

Recently, eutectic scintillators containing  $^6\text{Li}$  have been proposed for thermal neutron detection. Figure 1 shows a schematic of these eutectic scintillators, which consist of two phases: a neutron-capture phase, in which a nuclear transmutation reaction involving  $^6\text{Li}$  is performed, and a scintillator phase, in which the  $\alpha$ -rays and tritons are absorbed and visible light is generated. This eutectic scintillator allows for a higher concentration of  $^6\text{Li}$  than conventional single-crystal scintillators, thereby increasing the sensitivity to thermal neutrons.

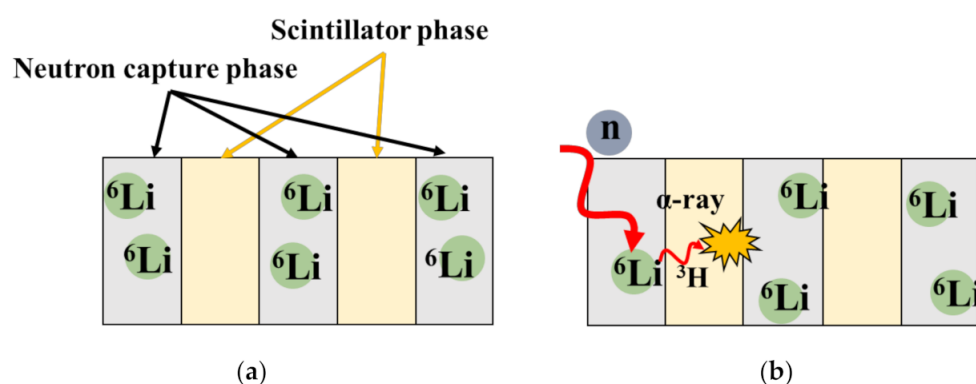


**Figure 1.** Schematic diagrams of (a) a eutectic scintillator for thermal neutron detection and (b) luminescence mechanism.

Our group has developed eutectic scintillators for thermal neutron detection, such as  $\text{Ce}^{3+}$ -activated bromide of  $\text{CeBr}_3/{}^6\text{LiBr}$  [13] and  $\text{Eu}^{2+}$ -activated chlorides of  $\text{Eu:BaCl}_2/{}^6\text{LiCl}$  [14] and  $\text{Eu:}{}^6\text{Li}_2\text{SrCl}_4/{}^6\text{LiCl}$  [15]. Some of them have been reported to exceed the scintillator properties of conventional single-crystal scintillators in terms of  $^6\text{Li}$  concentration and light yield. These results have encouraged us to continue exploring new materials for eutectic scintillators, which is crucial for the development of alternative thermal neutron detection [16].

In this study, new eutectics were developed by taking advantage of both the fast decay time of  $\text{Ce}^{3+}$  activation and the low density of chloride crystals. Here,  ${}^6\text{LiCl}$  was selected as the neutron capture phase and  $\text{K}_2\text{CeCl}_5$  and  $\text{CeCl}_3$  were used as the scintillator phases. The scintillation properties of  $\text{K}_2\text{CeCl}_5$  [17] and  $\text{CeCl}_3$  [18] have been reported as light yields of 31,000 and 46,000 photons/MeV under  $\gamma$ - or X-ray irradiation, decay times of 25 ns (69%), 861 ns (8%), 14  $\mu\text{s}$  (23%), and densities of 2.76 and 3.84 g/cm<sup>3</sup>, respectively [19]. The refractive index of each phase is an important parameter when using eutectics as optical materials. When the refractive index difference is large, the transparency is reduced and the light collection efficiency decreases. If the refractive index difference is small, the transparency such as that of single crystals can be obtained even in eutectic crystals and the light collection efficiency improves. The refractive index of the materials of interest in this study are  $\text{LiCl}$  (1.67@365 nm [20]),  $\text{K}_2\text{CeCl}_5$  (not reported),  $\text{CeCl}_3$  (2.2@365 nm [21]), and  $\text{SrCl}_2$  (1.66@488 nm [22]), respectively. For these combinations of crystalline phases, not only a binary eutectic of  $\text{K}_2\text{CeCl}_5/{}^6\text{LiCl}$  but also a ternary eutectic of  $\text{CeCl}_3/\text{SrCl}_2/{}^6\text{LiCl}$  was identified as a new attempt based on the phase diagram database. [23,24]. In a previous study, a  $\text{CeCl}_3/{}^6\text{LiCl}$  binary eutectic scintillator was reported [21]. The objective of this study was to investigate whether a change in eutectic structure and transparency could be improved by fabricating the ternary eutectic containing  $\text{SrCl}_2$  in addition to  $\text{LiCl}$ . Eutectics

of  $\text{K}_2\text{CeCl}_5/{}^6\text{LiCl}$  and  $\text{CeCl}_3/\text{SrCl}_2/{}^6\text{LiCl}$  were prepared using the Vertical Bridgman (VB) method and the phases were identified by scanning electron microscopy and powder X-ray diffraction measurements. The radioluminescence spectra under X-ray irradiation, cathodoluminescence spectra, and thermal neutron responses of the prepared eutectics were measured to evaluate their optical properties.

## 2. Materials and Methods

### 2.1. Crystal Growth

Eutectics were grown using the VB method. Each halide powder was weighted in a glove box of Ar atmosphere and according to the eutectic points of KCl (4N) 28.3 mol%,  $\text{CeCl}_3$  (4 N) 14.2 mol%, and LiCl (4 N) 57.5 mol% for  $\text{K}_2\text{CeCl}_5/{}^6\text{LiCl}$  and  $\text{CeCl}_3$  (4 N) 19.9 mol%,  $\text{SrCl}_2$  (4 N) 28.0 mol%, and LiCl (4 N) 52.1 mol% for  $\text{CeCl}_3/\text{SrCl}_2/{}^6\text{LiCl}$ , based on the phase diagrams of Refs. [23,24]. The mixed powders were fed into quartz ampoules with inner diameters of 6 mm. Because these halide powders are deliquescent, baking was carried out at 200 °C for at least 3 h in a vacuum to remove the water contained in the pristine powder. Subsequently, a cryopump was used to draw a vacuum down to  $10^{-5}$  Pa and then sealed. The sealed ampoule was heated using a Pt tube heater with a high-frequency coil and pulled down at a rate of 0.2 mm/min. In this study, rates applied in the previous literature [13–15] were selected in order to verify the potential of the eutectics as thermal neutron scintillators. The grown eutectics were cut and polished in the cross-section and growth direction using a wire saw in a dry room (humidity < 3%) to prevent deliquescence. The crystal phases were identified and their scintillation properties were evaluated.

### 2.2. Phase Identification

To observe the microstructure of the eutectic crystals, backscattered electron (BSE) images were obtained using a scanning electron microscope (SEM) (S-3400N, Hitachi, Japan and JSM-7800F, JEOL Ltd., Tokyo, Japan). Powder X-ray diffraction (XRD) measurements were performed for phase identification using a D8 DISCOVER (Bruker, MA, USA). The measurement conditions were  $10^\circ$ – $90^\circ$  and the X-ray source was a Cu-K $\alpha$  beam with a tube voltage of 40 kV and a tube current of 40 mA. To prevent the deliquescence of the halide eutectic crystals during the powder XRD measurement, the preparation process was performed in a dry room and a non-exposure cover to the atmosphere was used.

### 2.3. Scintillation Properties

Radioluminescence (RL) measurements were performed using an Ag source X-ray tube (30 kV, 130 mA) to measure the emission wavelength. A charge-coupled device (CCD) camera (iDus420-OE, Andor Technology, Belfast, UK) with a spectrometer (SR-163, Andor Technology, Belfast, UK) was used for the measurements. In addition, cathodoluminescence (CL) (MP-32 S, HORIBA, Kyoto, Japan) spectra were measured to determine the emission spectra of each phase of the eutectic. The light yields and decay times under  ${}^{252}\text{Cf}$  radioisotope irradiation of the prepared eutectics were evaluated. The eutectic scintillators were attached to a photomultiplier tube (PMT) (R7600-200, Hamamatsu, Shizuoka, Japan) with optical grease (KF-96H-60000CS, SHINETSU, Tokyo, Japan) and the signals were read. The sample and radiation source ( ${}^{252}\text{Cf}$ ) were spaced approximately 10 cm apart using a neutron moderator. To evaluate the light yield, the analog signals were acquired using a two-channel USB WaveCatcher module [25]. To measure the decay time, PMT was connected with an oscilloscope (TDS3035B, TEKTRONIX, Beaverton, OR, USA) directly.

## 3. Results and Discussion

### 3.1. Crystal Growth

The grown  $\text{K}_2\text{CeCl}_5/{}^6\text{LiCl}$  and  $\text{CeCl}_3/\text{SrCl}_2/{}^6\text{LiCl}$  eutectics are shown in Figure 2a,b, respectively. Figure 2c,d show photographs of 1 mm thick wafers of the respectively prepared eutectic crystals. As seen from the wafers' photographs, the grown eutectics has

optical transparency.  $\text{CeCl}_3/{}^6\text{LiCl}$  reported in previous studies is less transparent [21]. On the other hand, the addition of  $\text{SrCl}_2$  improved transparency, although quantitative evaluation is difficult.

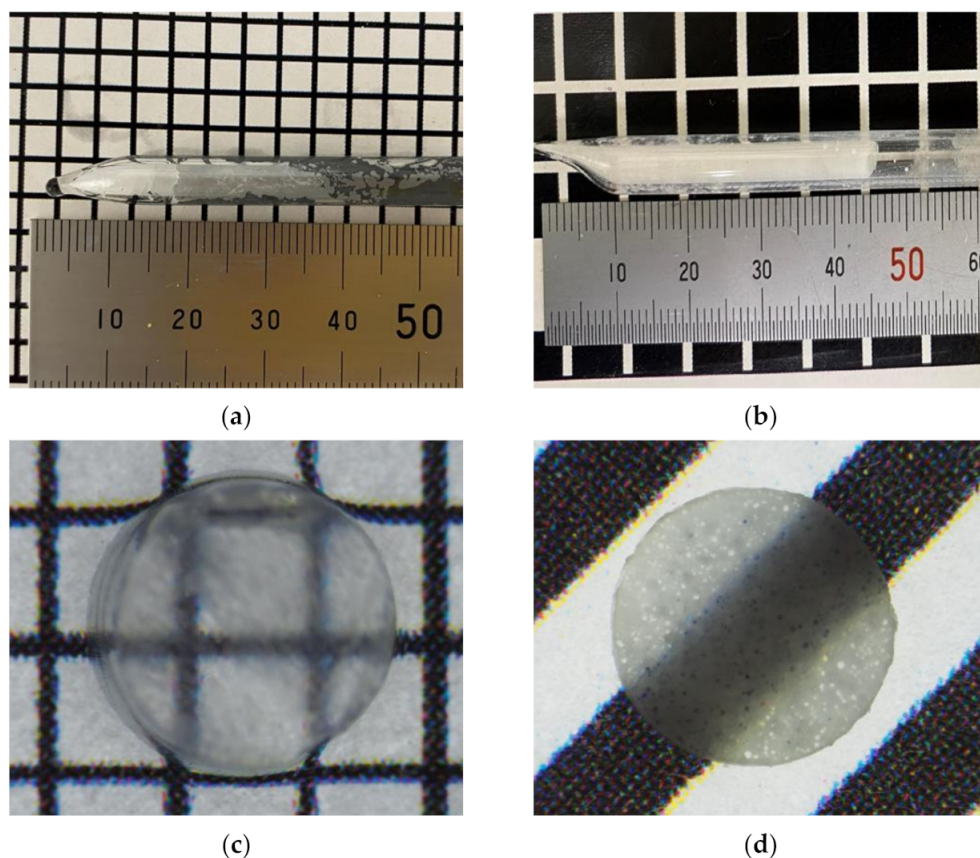
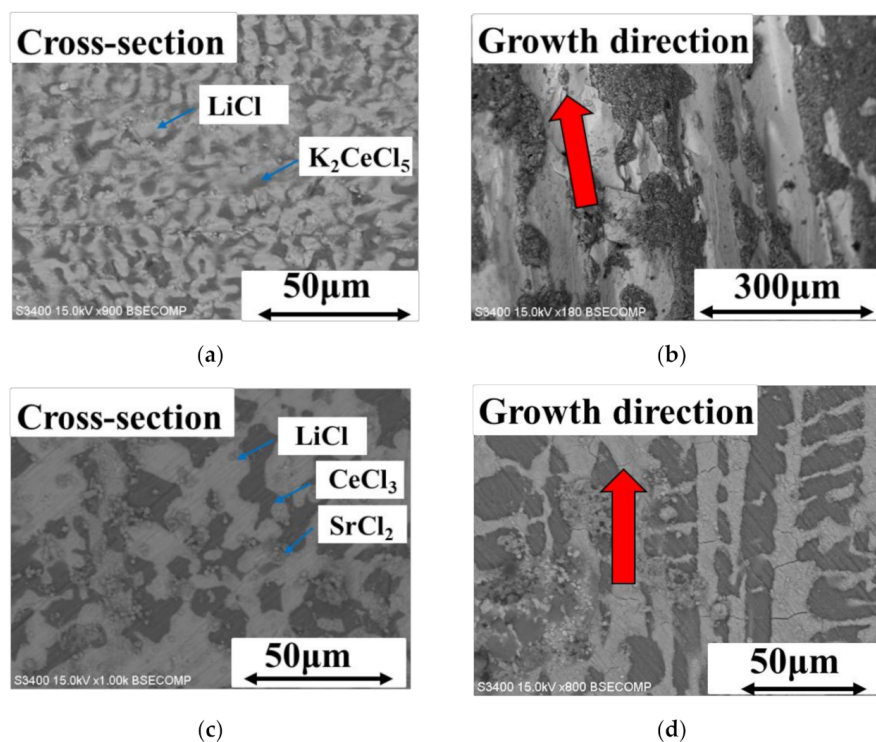


**Figure 2.** Photographs of growth eutectic crystals (a)  $\text{K}_2\text{CeCl}_5/\text{LiCl}$ , (b)  $\text{CeCl}_3/\text{SrCl}_2/\text{LiCl}$ , and 1 mm thick wafer of (c)  $\text{K}_2\text{CeCl}_5/\text{LiCl}$  and (d)  $\text{CeCl}_3/\text{SrCl}_2/\text{LiCl}$ .

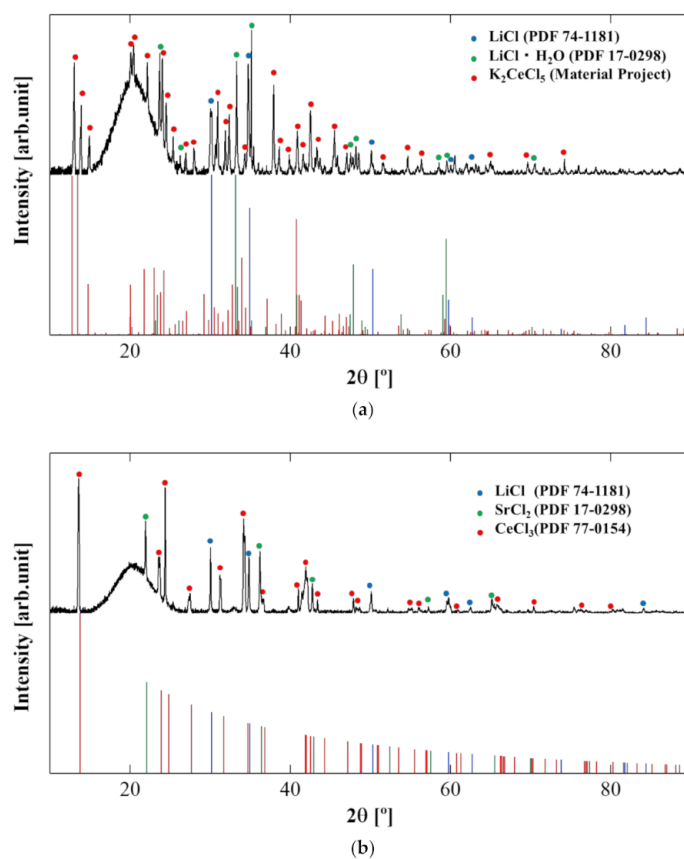
### 3.2. Phase Identification

Figure 3 shows the BSE images of the  $\text{K}_2\text{CeCl}_5/{}^6\text{LiCl}$  and  $\text{CeCl}_3/\text{SrCl}_2/{}^6\text{LiCl}$  eutectics in the cross-sectional and growth directions. The differences in atomic numbers contrasted in each phase and multiple phases were identified. Figure 4 shows the powder XRD results. In Figure 4a, two target phases,  $\text{K}_2\text{CeCl}_5$  (orthorhombic, Pnma, 62, Material Project [19]) and  $\text{LiCl}$  (cubic, Fm-3 m, 225, PDF 74-1181), were identified. Because  $\text{K}_2\text{CeCl}_5$  and  $\text{LiCl}$  are deliquescent, the  $\text{LiCl} \cdot \text{H}_2\text{O}$  (PDF 17-0298) peak of the tidal product was also present. The hydrate precipitation is thought to have occurred during crushing of the eutectics. Figure 4b shows the results for the  $\text{CeCl}_3/\text{SrCl}_2/{}^6\text{LiCl}$  eutectic. The three desired phases of  $\text{CeCl}_3$  (hexagonal, P63/m, 176, PDF 77-0154),  $\text{SrCl}_2$  (cubic, Fm-3 m, 225, PDF 06-0537), and  $\text{LiCl}$  were confirmed and both crystals with the desired eutectic composition were successfully obtained. The broad peak at approximately  $20^\circ$  is derived from the airtight package. The results of BSE images and powder XRD measurements show that in Figure 3a, the black area is  $\text{LiCl}$  and the white area is  $\text{K}_2\text{CeCl}_5$ , and in (c), the black area is  $\text{LiCl}$ , the gray area is  $\text{SrCl}_2$ , and the white area is  $\text{CeCl}_3$ . The particle sizes of  $\text{K}_2\text{CeCl}_5$  and  $\text{LiCl}$  in  $\text{K}_2\text{CeCl}_5/\text{LiCl}$  both are about  $10\ \mu\text{m}$  and of  $\text{CeCl}_3/\text{SrCl}_2/\text{LiCl}$  are about  $25\ \mu\text{m}$ ,  $5\ \mu\text{m}$ , and  $25\ \mu\text{m}$ , respectively.





**Figure 3.** BSE images of (a)  $K_2CeCl_5/LiCl$  cross-section and (b) growth direction and (c)  $CeCl_3/SrCl_2/LiCl$  cross-section and (d) growth direction.

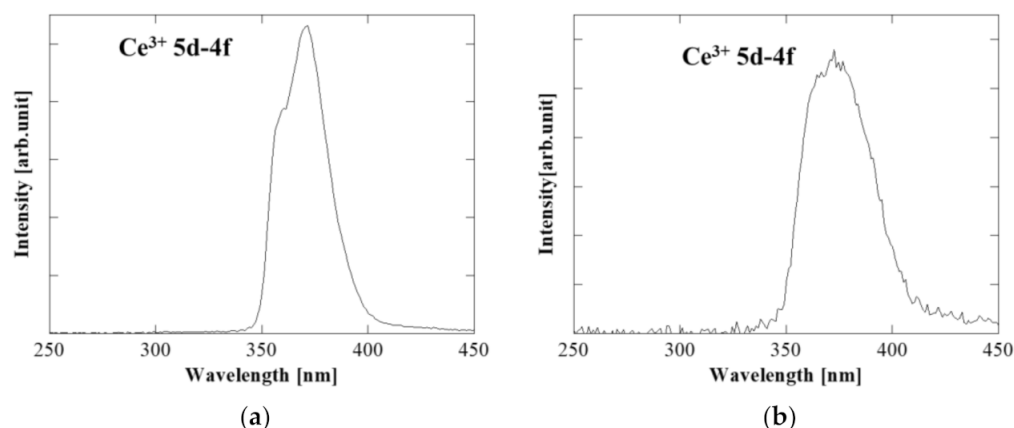


**Figure 4.** Powder XRD patterns of prepared (a)  $K_2CeCl_5/LiCl$  and (b)  $CeCl_3/SrCl_2/LiCl$ .

In the grown eutectic, the crystalline phase tended to elongate in the pull-down direction. In the wafer shown in Figure 2, there were variations in the transparent areas. This indicates that transparency was high in areas where the crystalline phase was uniformly elongated. Transparency is an important factor in scintillator applications and can be improved by optimizing the growth conditions and increasing the uniformity of the crystal phase elongation. In addition, each crystalline phase should consist of single grains. As shown in the past literature [26,27], each grain of eutectic is single grain in principle. It is difficult to submit evidence due to the difficulty of EBSD and other measurements in strongly hygroscopic samples.

### 3.3. Luminescence Properties

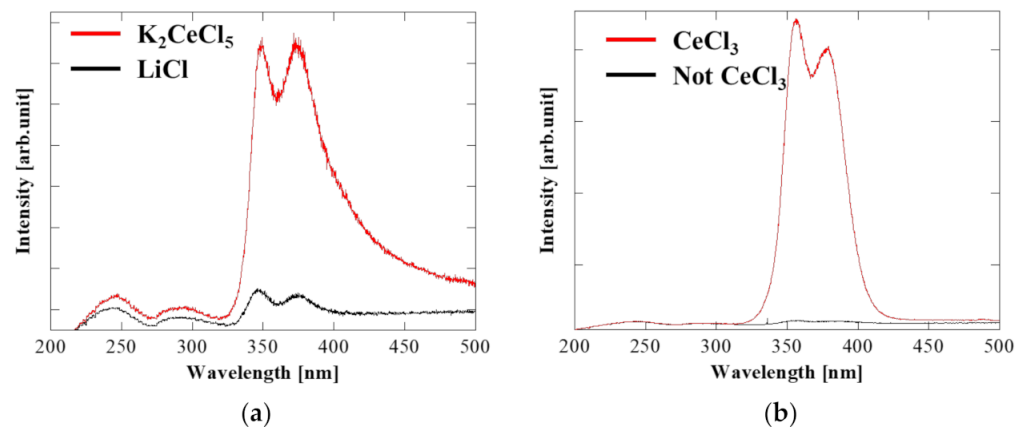
Figure 5 shows the results of the RL spectra under Ag-source X-ray tube irradiation. In both eutectics, emission spectra due to the 5d-4f transition of  $\text{Ce}^{3+}$  were obtained, peaking at approximately 380 nm. The emission wavelengths of  $\text{K}_2\text{CeCl}_5$  and  $\text{CeCl}_3$  correspond to those reported in previous studies [17,18].



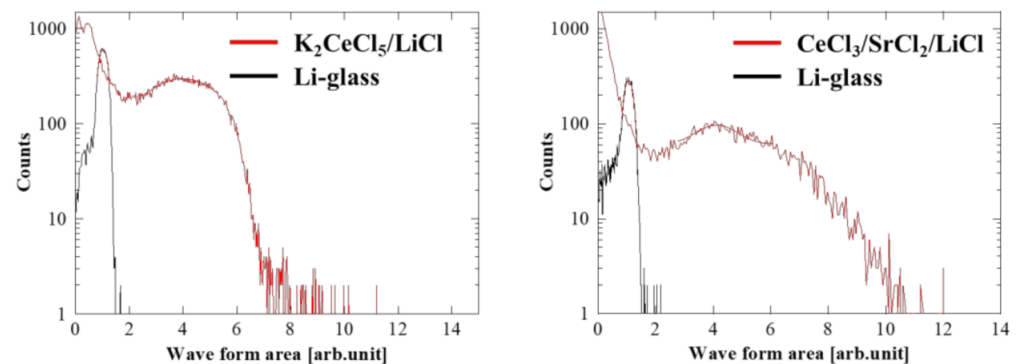
**Figure 5.** RL spectra under X-ray irradiation of prepared (a)  $\text{K}_2\text{CeCl}_5/\text{LiCl}$  and (b)  $\text{CeCl}_3/\text{SrCl}_2/\text{LiCl}$ .

Figure 6 shows the CL spectra for each phase. The red and black lines in Figure 6a show the emission spectra of the  $\text{K}_2\text{CeCl}_5$  and  $\text{LiCl}$  phases, respectively, under electron beam irradiation. The red and black lines in Figure 6b show the emission spectra of the  $\text{CeCl}_3$  and non- $\text{CeCl}_3$  phases, respectively. In both crystals, only the scintillator phase showed  $\text{Ce}^{3+}$  5d-4f emission in the 340–440 nm range and neither the  $\text{LiCl}$  phase nor the  $\text{SrCl}_2$  phase showed strong emission. There is a weak  $\text{Ce}^{3+}$  5d-4f emission peak in the  $\text{LiCl}$  phase and a long-wavelength shoulder in the  $\text{K}_2\text{CeCl}_5$  phase of  $\text{K}_2\text{CeCl}_5/{}^6\text{LiCl}$ . These may be due to the generation and erosion of  $\text{K}_2\text{CeCl}_5$  hydrates during the preparation process or the spreading of the electron beams. Two peaks at 240 and 280 nm were identified in both eutectics, which were considered background noise originating from the equipment setup. Both the RL peaks on the short wavelength side of the  $\text{Ce}^{3+}$  5d-4f emission were weaker compared with the CL. Since the scintillation light transmits through the sample in RL, it is considered to be an effect of self-absorption near the cutoff wavelength, as in the past report [28].

The pulse-height spectra of  $\text{K}_2\text{CeCl}_5/{}^6\text{LiCl}$  and  $\text{CeCl}_3/\text{SrCl}_2/{}^6\text{LiCl}$  under  ${}^{252}\text{Cf}$  radioisotope irradiation are shown in Figure 7a,b, respectively. A Li-glass standard (GS-20, Scintacor, Cambridge, UK), which has 6000 photons/neutron of light yield, was used as a reference [29]. The light yields of  $\text{K}_2\text{CeCl}_5/{}^6\text{LiCl}$  and  $\text{CeCl}_3/\text{SrCl}_2/{}^6\text{LiCl}$  showed to be 23,000 and 22,000 photons/neutron, respectively, which is 3.85 and 3.71 times higher than the Li-glass standard.



**Figure 6.** The CL spectra of prepared (a)  $K_2CeCl_5/LiCl$  and (b)  $CeCl_3/SrCl_2/LiCl$ .



**Figure 7.** Pulse-height spectra of prepared (a)  $K_2CeCl_5/LiCl$  and (b)  $CeCl_3/SrCl_2/LiCl$  under  $^{252}Cf$  irradiation.

The decay curves under  $^{252}Cf$  radioisotope irradiation were also measured and are shown in Figure 8. Decay times were calculated by fitting Equation (2) to the decay curve.

$$y = y_0 + \sum A_i \exp\left(-\frac{x - x_0}{\tau_i}\right) \quad (2)$$

The obtained decay times were  $\tau_1 = 4$  ns (3%) and  $\tau_2 = 66$  ns (97%) for  $K_2CeCl_5/{}^6LiCl$  and  $\tau_1 = 5$  ns (3%),  $\tau_2 = 51$  ns (42%), and  $\tau_3 = 566$  ns (55%) for  $CeCl_3/SrCl_2/{}^6LiCl$ . In both crystals, the 5d-4f fast emission of  $Ce^{3+}$  was the main emission. In the case of the  $K_2CeCl_5/{}^6LiCl$  eutectic, the decay time under neutron irradiation is slightly faster than that of the  $K_2CeCl_5$  single crystal under  $\gamma$ -ray irradiation [17]. This is assumed to be due to the substitution of  $Li^+$  into the  $K_2CeCl_5$  phase and the difference in response to neutron and  $\gamma$ -ray radiation. The decay time under  $\gamma$ -ray irradiation of the  $CeCl_3$  single crystal was reported to be 25 ns (69%), 869 ns (8%), and 14  $\mu$ s (23%) for the three components, while 20 ns was reported for the  $CeCl_3/LiCl$  binary eutectic, with no mention of lower decay components [18,30]. In the  $CeCl_3/SrCl_2/{}^6LiCl$  ternary eutectic, the decay components under neutron irradiation were faster than the  $CeCl_3$  single crystal and the component ratio was changed. This may be due to the substitution of  $Sr^{2+}$  and  $Li^+$  into the  $CeCl_3$  phase. The difference in response to neutron and  $\gamma$ -ray irradiation is also considered. The effects of substitution of other phases in eutectics can be studied by fabricating each single crystal with an intentional substitution of  $Sr^{2+}$  and  $Li^+$  and characterizing its scintillation properties by  $\gamma$ -ray excitation. However, it is not possible to evaluate the neutron response of Li-free single crystals. The scintillation properties of the prepared eutectics and common thermal neutron scintillators are listed in Table 1 [11,12,19,29,31]. The  $K_2CeCl_5/{}^6LiCl$  and  $CeCl_3/SrCl_2/{}^6LiCl$  eutectics showed higher light yields than Ce: LiCAF and Ce: CLYC.

Compared with the  $\text{CeCl}_3/{}^6\text{LiCl}$  binary eutectic, the transparency was improved in the  $\text{CeCl}_3/\text{SrCl}_2/{}^6\text{LiCl}$  ternary eutectic, although it is difficult to quantify. On the other hand, the light yield decreased probably due to absorption of  $\alpha$ -rays and tritons in the non-luminescent  $\text{SrCl}_2$ . The  $\text{CeCl}_3/\text{SrCl}_2/{}^6\text{LiCl}$  eutectic cannot be considered as a promising scintillator because of the trade-off between the decrease in  ${}^6\text{Li}$  concentration and light yield and transparency. However, we believe that this result shows the possibility of controlling transparency and eutectic structure by extending from binary systems to ternary systems. In particular, the  $\text{K}_2\text{CeCl}_5/{}^6\text{LiCl}$  eutectic showed a fast decay time comparable to that of Eu: LiCAF and Ce: CLYC, the lowest density, and the highest  ${}^6\text{Li}$  concentration among these scintillators. Owing to its excellent performance,  $\text{K}_2\text{CeCl}_5/{}^6\text{LiCl}$  is a promising scintillator for neutron detection applications.

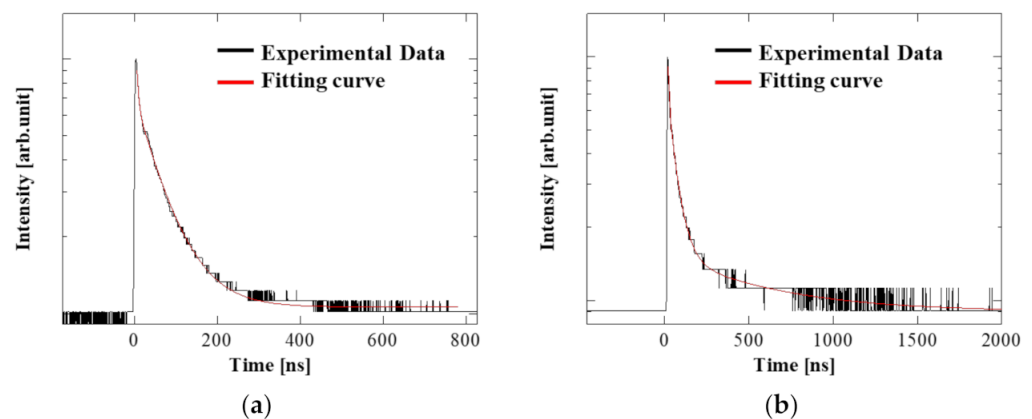


**Figure 8.** Decay curves of prepared (a)  $\text{K}_2\text{CeCl}_5/\text{LiCl}$  and (b)  $\text{CeCl}_3/\text{SrCl}_2/\text{LiCl}$  under  ${}^{252}\text{Cf}$  irradiation.

**Table 1.** Scintillation properties of the prepared eutectics and common thermal neutron scintillators.

	Activator	Li Concentration (mol/cm <sup>3</sup> )	Density (g/cm <sup>3</sup> )	Hygroscopicity	Light Yield (Photons/Neutron)	Decay Time (ns)
$\text{K}_2\text{CeCl}_5/{}^6\text{LiCl}$	Ce	0.035	2.65 [19]	high	23,000	4, 66
$\text{CeCl}_3/\text{SrCl}_2/{}^6\text{LiCl}$	Ce	0.025	3.02 [19]	high	22,000	5, 51, 566
LiCAF	Ce	0.015	2.9 [29]	No	4200 [11]	38 [11]
LiCAF	Eu	0.015	2.9 [29]	No	29,000 [30]	1150 [31]
CLYC	Ce	0.006	3.3 [29]	Little	14,400 [12]	900 [12]

As shown in the previous study [27], the size of each grain is refined by increasing the growth rate according to the Hunt–Jackson rule. This allows  $\alpha$ -rays and tritons generated by transmutation reactions in the Li-containing phase to be transferred to the scintillator phase without energy loss; thus, an increase in light yield can be expected. This study pioneered the testing of  $\text{K}_2\text{CeCl}_5/{}^6\text{LiCl}$  and  $\text{CeCl}_3/\text{SrCl}_2/{}^6\text{LiCl}$  as promising neutron scintillators with transparency, considering their refractive index; although, a refractive index value of  $\text{K}_2\text{CeCl}_5$  does not exist in the database. For further evaluation as a neutron scintillator, the relationship between the pull-down rate, the size of the eutectic phase, and the transparency and light yield should be investigated and optimized in the future, aiming at the practical use as a transparent eutectic with a large aperture. To evaluate the uniformity of the eutectic phase, we need to fabricate a prototype with a size of about 1 inch in diameter, which requires more expensive raw materials and more time for the fabrication. We would like to conduct the following studies: larger size and higher performance, trial manufacture and refractive index evaluation of  $\text{K}_2\text{CeCl}_5$  single crystals, and more detailed neutron response evaluation using large transparent eutectics such as pulse shape discrimination performance and  $\alpha/\gamma$  ratio.



#### 4. Conclusions

In this study,  $\text{K}_2\text{CeCl}_5/{}^6\text{LiCl}$  and  $\text{CeCl}_3/\text{SrCl}_2/{}^6\text{LiCl}$  eutectic scintillators for thermal neutrons were prepared using the Vertical Bridgman (VB) method. The desired phase was confirmed in both crystals using SEM and powder XRD measurements. Optical characterization of the crystals confirmed that 5d-4f was derived from  $\text{Ce}^{3+}$  luminescence. The light yields under  ${}^{252}\text{Cf}$  neutron source irradiation of  $\text{K}_2\text{CeCl}_5/{}^6\text{LiCl}$  and  $\text{CeCl}_3/\text{SrCl}_2/{}^6\text{LiCl}$  were measured to be 23,000 and 22,000 photons/neutron, respectively. The decay times under  ${}^{252}\text{Cf}$  irradiation were  $\tau_1 = 4$  ns (3%) and  $\tau_2 = 66$  ns (97%) for  $\text{K}_2\text{CeCl}_5/{}^6\text{LiCl}$  and  $\tau_1 = 5$  ns (3%),  $\tau_2 = 51$  ns (42%), and  $\tau_3 = 561$  ns (55%) for  $\text{CeCl}_3/\text{SrCl}_2/{}^6\text{LiCl}$ . The  ${}^6\text{Li}$  concentration, which is an important factor in scintillators for thermal neutron detection, was  $0.035$  mol/ $\text{cm}^3$  for  $\text{K}_2\text{CeCl}_5/{}^6\text{LiCl}$  and  $0.025$  mol/ $\text{cm}^3$  for  $\text{CeCl}_3/\text{SrCl}_2/{}^6\text{LiCl}$ , which is higher than that of typical single-crystal scintillators for thermal neutron detection, such as Ce: LiCAF ( $0.015$  mol/ $\text{cm}^3$ ) and Ce: CLYC ( $0.006$  mol/ $\text{cm}^3$ ). Therefore, the developed eutectic scintillators are promising materials with high sensitivity and scintillator properties for thermal neutrons.

**Author Contributions:** Conceptualization, R.Y. and K.K.; methodology, R.Y. and K.K.; formal analysis, R.Y. and M.Y.; investigation, R.Y. and R.S.; writing—original draft preparation, R.Y.; writing—review and editing, K.K., M.Y., Y.T., N.K., R.S., T.H. (Takahiko Horiai), R.M., K.J.K., V.V.K., A.Y. (Akihiro Yamaji), S.K., Y.Y., H.S., S.T., Y.O., T.H. (Takashi Hanada), and A.Y. (Akira Yoshikawa); supervision, A.Y. (Akihiro Yamaji); project administration, K.K.; funding acquisition, K.K. All authors have read and agreed to the published version of the manuscript.

**Funding:** this work was partially supported by KAKENHI, Japan Society for the Promotion of Science, grant numbers 18H01222, 19H00672, 20K20488, 17H06159, 19H00881, 19K12626.

**Acknowledgments:** Authors would like to thank the following persons for their support: Shigeru Otsuka and Masahiro Fukukawa at the University of Tokyo and the Nanotechnology Platform project by the Ministry of Education, Culture, Sports, Science, and Technology of Japan and Keiko Toguchi, Megumi Sasaki and Kuniko Kawaguchi at Institute for Materials Research, Tohoku University. We also would like to thank Editage ([www.editage.com](http://www.editage.com)) for English language editing (21 October 2022).

**Conflicts of Interest:** The authors declare no conflict of interest. The funders had no role in the design of the study; in the collection, analyses, or interpretation of data; in the writing of the manuscript; or in the decision to publish the results.

#### References

1. Moss, R.L. Critical review, with an optimistic outlook, on boron neutron capture therapy (BNCT). *Appl. Radiat. Isot.* **2014**, *88*, 2–11. [[CrossRef](#)] [[PubMed](#)]
2. Kouzes, R.T.; Ely, J.H.; Erikson, L.E.; Kernan, W.J.; Lintereur, A.T.; Siciliano, E.R.; Stephens, D.L.; Stromswold, D.C.; Van Ginhoven, R.M.; Woodring, M.L. Neutron detection alternatives to  ${}^3\text{He}$  for national security applications. *Nucl. Instrum. Methods Phys. Res. Sect. A Accel. Spectrometers Detect. Assoc. Equip.* **2010**, *623*, 1035–1045. [[CrossRef](#)]
3. Blakeley, M.P.; Langan, P.; Niimura, N.; Podjarny, A. Neutron crystallography: Opportunities, challenges, and limitations. *Curr. Opin. Struct. Biol.* **2008**, *18*, 593–600. [[CrossRef](#)]
4. Lehmann, E.; Mannes, D.; Kaestner, A.; Grünzweig, C. Recent applications of neutron imaging methods. *Phys. Procedia* **2017**, *88*, 5–12. [[CrossRef](#)]
5. Kardjilov, N.; Manke, I.; Woracek, R.; Hilger, A.; Banhart, J. Advances in neutron imaging. *Mater. Today* **2018**, *21*, 652–672. [[CrossRef](#)]
6. Ziesche, R.F.; Kardjilov, N.; Kockelmann, W.; Brett, D.J.L.; Shearing, P.R. Neutron imaging of lithium batteries. *Joule* **2022**, *6*, 35–52. [[CrossRef](#)]
7. Ravazzani, A.; Foglio Para, A.; Jaime, R.; Looman, M.; Marín Ferrer, M.; Peerani, P.; Schillebeeckx, P. Characterisation of  ${}^3\text{He}$  Proportional Counters. *Radiat. Meas.* **2006**, *41*, 582–593. [[CrossRef](#)]
8. Kouzes, R.T.; Ely, J.H.; Lintereur, A.T.; Siciliano, E.R.; Woodring, M.L. *BF<sub>3</sub> Neutron Detector Tests*; Rep. PNNL-19050; Pacific Northwest National Lab: Richland, WA, USA, 2009.
9. Glenn, F.K. *Radiation Detection and Measurement*; John Wiley & Sons: Hoboken, NJ, USA, 2010.
10. Kawaguchi, N.; Yanagida, T.; Novoselov, A.; Kim, K.J.; Fukuda, K.; Yoshikawa, A. Neutron responses of  $\text{Eu}^{2+}$  activated LiCaAlF<sub>6</sub> scintillator. In Proceedings of the 2008 IEEE Nuclear Science Symposium Conference Record, Dresden, Germany, 19–25 October 2008; pp. 1174–1176.

11. Yoshikawa, A.; Yanagida, T.; Yokota, Y.; Kawaguchi, N.; Ishizu, S.; Fukuda, K.; Licaf, C.L. Single crystal growth, optical properties and neutron response of Ce<sup>3+</sup> doped LiCaAlF<sub>6</sub>. *IEEE Trans. Nucl. Sci.* **2009**, *56*, 3796–3799. [\[CrossRef\]](#)
12. Glodo, J.; Higgins, W.M.; Van Loef, E.V.D.; Shah, K.S. Scintillation properties of 1 inch Cs<sub>2</sub>LiYCl<sub>6</sub>:Ce crystals. *IEEE Trans. Nucl. Sci.* **2008**, *55*, 1206–1209. [\[CrossRef\]](#)
13. Ryuga, Y.; Takizawa, Y.; Kamada, K.; Yoshino, M.; Kim, K.J.; Murakami, R.; Shoji, Y.; Kochurikhin, V.V.; Yoshikawa, A. Growth and scintillation properties of LiBr/CeBr<sub>3</sub> eutectic scintillator for neutron detection. *J. Cryst. Growth* **2021**, *61*, 576.
14. Takizawa, Y.; Kamada, K.; Yoshino, M.; Yajima, R.; Kim, K.J.; Kochurikhin, V.V.; Yoshikawa, A. Growth of 6Li-enriched LiCl/BaCl<sub>2</sub> eutectic as a novel neutron scintillator. *Jpn. J. Appl. Phys.* **2022**, *61*, SC1038. [\[CrossRef\]](#)
15. Kutsuzawa, N.; Takizawa, Y.; Kamada, K.; Yoshino, M.; Kim, K.J.; Murakami, R.; Shoji, Y.; Kochurikhin, V.V.; Yoshikawa, A. Growth and scintillation properties of Eu-doped LiCl/Li<sub>2</sub>SrCl<sub>4</sub> eutectic scintillator for neutron detection. *J. Cryst. Growth* **2021**, *576*, 126373. [\[CrossRef\]](#)
16. Takizawa, Y.; Kamada, K.; Yoshino, M.; Kim, K.J.; Yamaji, A.; Kurosawa, S.; Yokota, Y.; Sato, H.; Toyoda, S.; Ohashi, Y.; et al. Growth and scintillation properties of Ce doped 6LiBr/LaBr<sub>3</sub> eutectic scintillator for neutron detection. *Nucl. Instrum. Methods Phys. Res. Sect. A Accel. Spectrometers Detect. Assoc. Equip.* **2022**, *1028*, 166384. [\[CrossRef\]](#)
17. Roy, U.N.; Groza, M.; Cui, Y.; Burger, A.; Cherepy, N.; Friedrich, S.; Payne, S.A. K<sub>2</sub>CeCl<sub>5</sub>: A new scintillator material. *Nucl. Instrum. Methods Phys. Res. Sect. A Accel. Spectrometers Detect. Assoc. Equip.* **2007**, *579*, 46–49. [\[CrossRef\]](#)
18. Van Loef, E.V.D.; Dorenbos, P.; Van Eijk, C.W.E.; Krämer, K.; Güdel, H.U. Scintillation properties of LaCl<sub>3</sub>:Ce<sup>3+</sup> Crystals: Fast, efficient, and high-energy resolution scintillators. *IEEE Trans. Nucl. Sci.* **2001**, *48*, 341–345. [\[CrossRef\]](#)
19. Materials Project. Available online: <https://materialsproject.org/> (accessed on 8 June 2022).
20. Li, H.H. Refractive Index of Alkali Halides and Its Wavelength and Temperature Derivatives. *J. Phys. Chem. Ref. Data.* **1976**, *5*, 329. [\[CrossRef\]](#)
21. Cheng, S.; Hunneke, R.E.; Tian, M.; Lukosi, E.; Zhuravleva, M.; Melcher, C.L.; Wu, Y. Self-Assembled NaLiCl-CeCl<sub>3</sub> Directionally Solidified Eutectics for Thermal Neutron Detection. *CrystEngComm* **2020**, *22*, 3269–3273. [\[CrossRef\]](#)
22. An, C.-X. Determination of the elastic constants of SrCl<sub>2</sub> by Brillouin scattering and study of their variations with temperature. *Phys. Stat. Sol.* **1977**, *43*, K69–K72. [\[CrossRef\]](#)
23. Qiao, Z.Y.; Xing, X.R. Construction and thermodynamic analysis of molten salt phase diagrams of systems containing rare earth chlorides. *Mater. Sci. Forum* **1991**, *73–75*, 217–226. [\[CrossRef\]](#)
24. He, M.; Lu, G.; Kang, Z.; Zhang, Y. Thermodynamic assessment of the LiCl-KCl-CeCl<sub>3</sub> system. *Calphad Comput. Coupling Phase Diagr. Thermochem.* **2015**, *49*, 1–7. [\[CrossRef\]](#)
25. Breton, D.; Delagnes, E.; Maalmi, J.; Rusquart, P. The WaveCatcher family of SCA-based 12-Bit 3.2-GS/s fast digitizers. In Proceedings of the 2014 19th IEEE-NPSS Real Time Conference, Nara, Japan, 30 April 2015; pp. 1–8.
26. Yoshiharu, W. Unidirectional Solidification of Oxide Eutectic Ceramics. *Jpn. Assoc. Cryst. Growth* **1999**, *26*, 107–117.
27. Takizawa, Y.; Kamada, K.; Kutsuzawa, N.; Yoshino, M.; Yamamoto, S.; Jin Kim, K.; Murakami, R.; Kochurikhin, V.V.; Yoshikawa, A. The Scintillation Performance of One-Inch Diameter CsI/CsCl/NaCl Eutectics Grown by the Czochralski Method. *J. Cryst. Growth.* **2021**, *572*, 126266. [\[CrossRef\]](#)
28. Alekhin, M.S.; Weber, S.; Krämer, K.W.; Dorenbos, P. Optical Properties and Defect Structure of Sr<sup>2+</sup> Co-Doped LaBr<sub>3</sub>:5%Ce Scintillation Crystals. *J. Lumin.* **2014**, *145*, 518–524. [\[CrossRef\]](#)
29. Dorenbos, P.; Van Eijk, C.W.E.; Bessi, A. Inorganic Thermal-Neutron Scintillators. *Nucl. Instrum. Methods Phys. Res. Sect. A Accel. Spectrometers Detect. Assoc. Equip.* **2004**, *529*, 260–267.
30. Rowe, E.; Tupitsyn, E.; Bhattacharya, P.; Matei, L.; Groza, M.; Buliga, V.; Atkinson, G.; Burger, A. Growth of KPb<sub>2</sub>Cl<sub>5</sub> and K<sub>2</sub>CeCl<sub>5</sub> for Gamma Ray Detection Using Vertical Bridgman Method. *J. Cryst. Growth.* **2014**, *393*, 156–158. [\[CrossRef\]](#)
31. Yanagida, T.; Kawaguchi, N.; Fujimoto, Y.; Fukuda, K.; Yokota, Y.; Yamazaki, A.; Watanabe, K.; Pejchal, J.; Uritani, A.; Iguchi, T.; et al. Basic study of Europium doped LiCaAlF<sub>6</sub> scintillator and Its capability for thermal neutron imaging application. *Opt. Mater.* **2011**, *33*, 1243–1247. [\[CrossRef\]](#)